Catalysis Communications 50 (2014) 44–48

Contents lists available at ScienceDirect

Catalysis Communications

journal homepage: www.elsevier.com/locate/catcom

Short Communication

Fabrication of NiFe layered double hydroxides using urea hydrolysis—Control of interlayer anion and investigation on their catalytic performance

Xu Wu, Yali Du, Xia An, Xianmei Xie *

College of Chemistry and Chemical Engineering, Taiyuan University of Technology, Taiyuan 030024, PR China

ARTICLE INFO

Article history:
Received 14 January 2014
Received in revised form 23 February 2014
Accepted 25 February 2014
Available online 4 March 2014

Keywords:
Urea hydrolysis
$NiFeNO_3$-LDH
$NiFeCO_3$-LDH
Catalysis
Benzoin ethyl ether

ABSTRACT

NiFe layered double hydroxides (NiFe-LDHs) intercalated with nitrate and carbonate anion were synthesized by urea hydrolysis. The aging time and the molar ratio of NO_3^-/urea were varied in order to identify suitable parameters, which control the interlayer anion (nitrate or carbonate) and crystal structure of the final products. The prepared samples were applied to the one-pot synthesis of benzoin ethyl ether from benzaldehyde and ethanol. NiFe–NO_3-LDH presented excellent catalytic activity, different from NiFe–CO_3-LDH which showed none catalytic activity at all.

1. Introduction

Layered double hydroxides (LDHs), also known as hydrotalcite-like compounds, are a family of anionic clays with three-dimensional networks. The structure of the LDHs is very similar to that of brucite $Mg(OH)_2$, in which each magnesium cation is octahedrally surrounded by hydroxyls. The resulting octahedron shares edges to form infinite sheets having no net charge [1,2]. In recent years, based on these structural characteristics, LDHs have attracted much attention in the development of new environment friendly catalysts [3–8].

Among all the studies covering this field, as a common feature, Al-based LDHs are always the mainly concerns [9–13]. Nowadays, with the research of layered double hydroxides in depth, as one member of LDH family, the catalytic performances of NiFe-LDHs have been drawing attentions of investigators [14–19].

As is well-known, catalytic activity is often ascribed to the presence of defect surface sites with unusually low coordination number, or ensembles of contiguous surface sites [20]. To trace the origin of these defects, the preparation method closely related with the catalytic behavior of the catalysts is an essential influencing factor. In view of this, numerous researchers have been endeavoring in exploration on synthesis procedure of NiFe-LDHs [21,22]. For example, Saiah et al. reported NiFe–CO_3-LDH synthesized by co-precipitation method [23]; Duan et al. prepared NiFe layered double hydroxide by decomposition of ammonium carbonate [24]; Liu et al. obtained NiFe–CO_3-LDH with high crystallinity and well-defined hexagon using urea as hydrolysis agent and trisodium citrate ($C_6H_5Na_3O_7 \cdot H_2O$) as chelating reagent [25]; Forano et al. obtained layered double hydroxide by enzymatic decomposition of urea [26]. Although NiFe-LDHs with different structures were prepared by diverse synthesis process, however, until now, little discussion was focused on interlayer ions in NiFe-LDHs. Furthermore, whether different interlayer ions of NiFe-LDHs will have effect on their catalytic performances have not been involved in the relevant reports yet.

Given the abovementioned, in the present work, we successfully prepared NiFe-LDHs by urea hydrolysis with seriously monitoring the preparation process. Particularly worth mentioning, NiFe–NO_3-LDH (nitrate as the interlayer anions), $Ni(HCO_3)_2$ and NiFe–CO_3-LDH (carbonate as the interlayer anions) were acquired orderly along with pH value and aging time altering. Especially, as environmentally friendly heterogeneous catalysts, NiFe-LDHs with different structures were introduced to the one-step synthesis of benzoin ethyl ether from benzaldehyde and ethanol to evaluate their catalytic performances [27,28]. Noticeably, these two kinds intercalated NiFe-LDHs presented totally different catalytic activities. Furthermore, the reason causing this distinct catalytic property of NiFe–NO_3-LDH and NiFe–CO_3-LDH was also discussed.

* Corresponding author. Tel.: +86 351 6018528.
E-mail addresses: s2003707@163.com, wuxu@tyut.edu.cn (X. Xie).

http://dx.doi.org/10.1016/j.catcom.2014.02.024
1566-7367/

Scheme 1.

2. Experimental

2.1. Preparation and characterization of the samples

NiFe-LDHs were prepared by urea hydrolysis. The corresponding ratios of urea solution and the mixed solution with 1.0 mol/L $Ni(NO_3)_2 \cdot 6H_2O$ and 0.5 mol/L $Fe(NO_3)_3 \cdot 9H_2O$ were added into a beaker. The mixtures were stirred for 30 min and then hydrothermally treated at 110 °C for 3–48 h, followed by cooling down the autoclave to room temperature. After measuring the pH value, the samples were dried at 80 °C in an air oven overnight.

Powder X-ray diffraction (XRD) patterns of the synthesized products were recorded on Rigaku D/max-2500 instrument (40 kV, 100 mA) using Cu Kα radiation at a scanning speed of 8° (2θ)/min, with the scanning territory 5–65°.

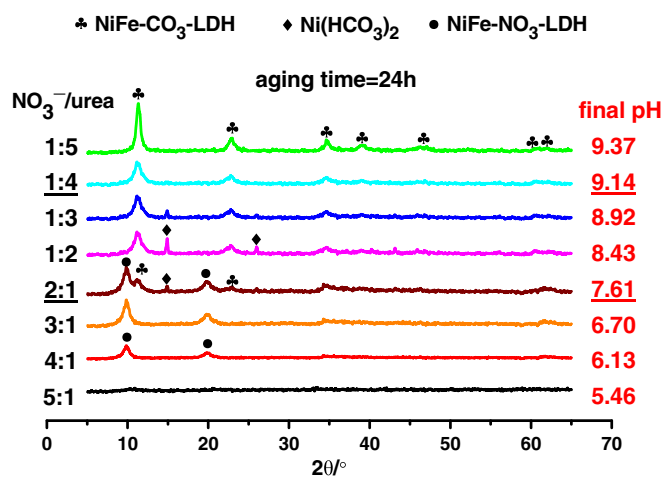

Fig. 1. XRD patterns of products with different starting concentrations of urea.

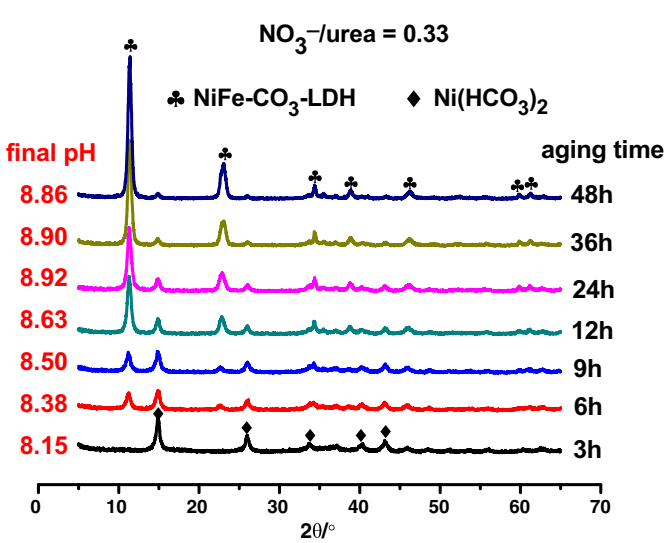

Fig. 2. XRD patterns of products when NO_3^-/urea = 0.33.

2.2. Typical procedure for synthesis of benzoin ethyl ether

A three-neck flask installed with a condenser and a thermometer was fixed in DF-101S magnetic stirred water bath, and then definite dosage of benzaldehyde, ethanol and NiFe-LDH catalyst (pretreatment under the condition of 423 K with N_2 flashing for 2 h) was added. After the reaction proceeded for a certain time at a constant temperature and normal pressure, the reaction mixture was analyzed using an HP (C6890A = 5973MSD) gas chromatograph equipped with a FFAP column (30 m ∗ 0.32 mm ∗ 0.5 μm) and an FID detector [9]. The main involved reaction formula is shown as Scheme 1.

3. Results and discussion

3.1. Catalyst characteristics

In urea hydrolysis method, the synthesis process and the products are susceptible to the pH value. However, the final pH value of the synthesis mixture can be influenced by modulating the aging time and the initial molar ratio of NO_3^-/urea [29]. Therefore, we focused on the impact of these two factors on the products, using XRD to analyze the crystal structure and phase composition of the obtained products.

3.1.1. Effects of NO_3^-/urea molar ratio

The XRD patterns for different initial concentrations of urea with aging time being 24 h were displayed in Fig. 1. As explicitly revealed in Fig. 1, three species gradually appeared with pH value varying. Noticeably, if the urea concentration is too low (higher molar ratio of NO_3^-/urea) to result in final pH value below 6, the NiFe-LDHs cannot be obtained. The possible factors related to this may be as follows: generally, amorphous $Fe(OH)_3$ initially formed in the aqueous solution, with further addition of the base, $Fe(OH)_3$ gradually converted to NiFe-HTLcs resultantly. However, the very low solubility of $Fe(OH)_3$ likely made the transformation of pH value from $Fe(OH)_3$ to NiFe-HTLcs close to 6 whereat Ni^{2+} ion deposits in the solution.

When the concentrations of urea were relatively high (lower molar ratio of NO_3^-/urea) to make final pH value around 9, NiFe–CO_3-LDH appeared; however, when at too low concentrations of reactants and pH value nearby 6.5, it is completely another case that the outcome became NiFe–NO_3-LDH. That is, when the concentrations of urea shifting from low to high, the product altered from NiFe–NO_3-LDH to NiFe–CO_3-LDH along with the arising of $Ni(HCO_3)_2$ during the mediate conversion

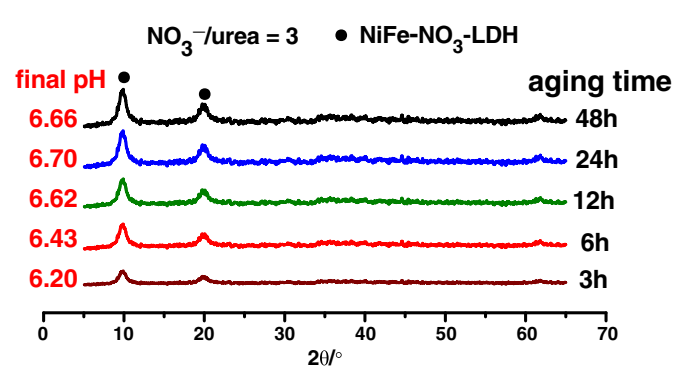

Fig. 3. XRD patterns of products when NO_3^-/urea = 3.

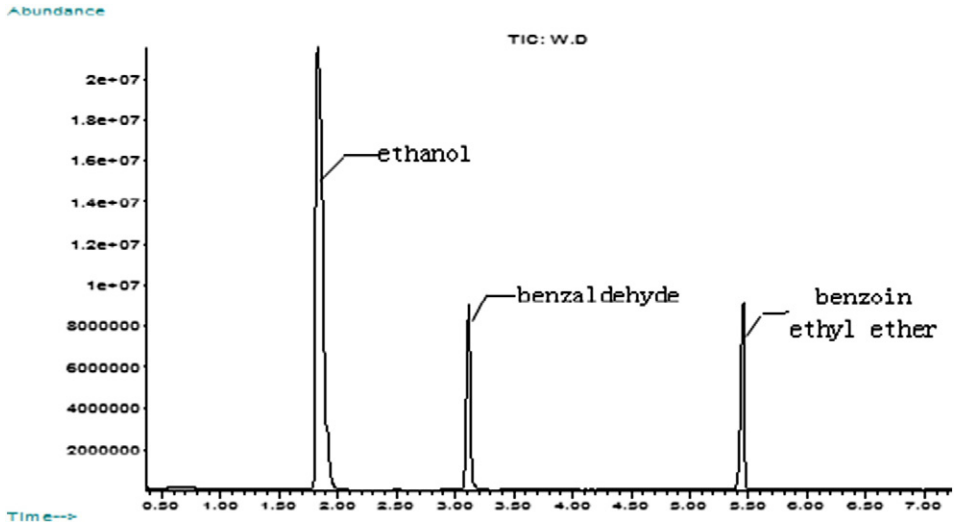

Fig. 4. Chromatogram analysis of the reaction mixture with NiFe–NO_3-LDH as the catalyst.

process. Briefly speaking, different products appeared under different reaction conditions. The reason for the appearance of this phenomenon lied in the transforming of urea concentrations which caused variation of pH value. Initially, at lower pH value, few carbonate could exist in the synthesis mixture so that nitrate would be the main compound available as interlayer anions. As carbonate ions possessing priority to nitrate ions in entering the interlayer, with pH value rising, as the ratio of CO_3^{2-}/NO_3^- reached a threshold level to create sufficient driving force to exclude nitrate from the reaction products. Thus, NiFe–CO_3-LDH began to emerge. Continually lifting of pH value brought about the mushrooming of CO_3^{2-} and thus NiFe–CO_3-LDH became the unique product. Furthermore, in comparison with NiFe–CO_3-LDH, the main diffraction peak of NiFe–NO_3-LDH in Fig. 1 moved slightly to lower angle direction, indicating the widening of interlayer space. All these abovementioned traits of the products might have an effect on their catalytic performances.

3.1.2. Effects of aging time

The XRD patterns of the products with different hydrothermal treatment times at NO_3^-/urea being 0.33 were shown in Fig. 2. After aging for 3 h, the diffraction peaks are indexed to $Ni(HCO_3)_2$, agreeing well with standard powder diffraction patterns (JCPDS#:1520782). Ranging from 6 h to 48 h, the diffraction peaks of $Ni(HCO_3)_2$ became lower and lower till disappearing, followed by a new diffraction peak appearing gradually and becoming sharper and sharper. A set of reflection appeared at 2θ angles of 11.5°,23.1°,34.4°, 38.9°, 46.3°, 59.9° and 61.2°, which can be well indexed to (003), (006), (012), (015), (018), (110) and (113) of NiFe–CO_3-LDH, respectively. Obviously, diffraction peaks of NiFe–CO_3-LDH are narrow and sharp, exhibiting excellent symmetry. No other crystalline phases were detected, suggesting that NiFe–CO_3-LDH with unique phase was obtained after hydrothermally treatment for 48 h at 110 °C. These phenomena evidently manifest that the composition of the products kept varying with the reaction proceeding and shifting from $Ni(HCO_3)_2$ to NiFe–CO_3-LDH in the synthesis process. The reason causing this shift may be as follows: firstly, low concentration of urea permitted the abundant existence of HCO_3^- till meeting the conditions to form $Ni(HCO_3)_2$; secondly, when urea concentration was high, hydroxyl, deriving from the urea decomposition, would interfere with the solubility equilibrium of $Ni(HCO_3)_2$ by

Table 1
Catalytic performance of NiFe–CO_3-LDH and NiFe–NO_3-LDH.

Sample	Conversion	Selectivity
NiFe–CO_3-LDH	0%	0%
NiFe–NO_3-LDH	51.5%	100%

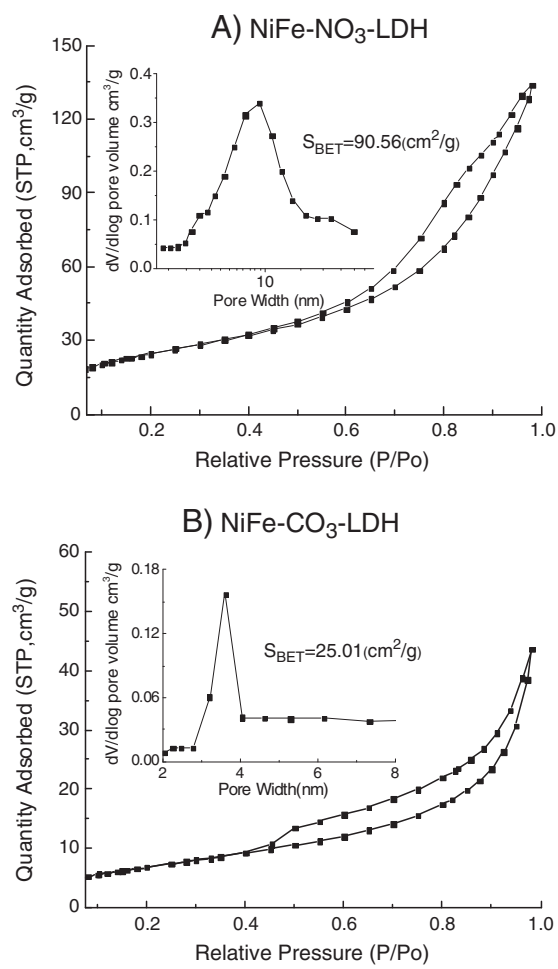

Fig. 5. N_2 adsorption–desorption isotherms and pore size distributions (inset) of NiFe-LDH.

consuming HCO_3^- and thus generating CO_3^{2-}. With the time going, the growing speed of pH value slowed down, $Ni(HCO_3)_2$ gradually transformed to NiFe − CO_3-LDH. All the involved reactions were given in sequence as follows:

$$CO(NH_2)_2 + 2H_2O \rightarrow 2NH_4^+ + CO_3^{2-} \quad (NH_4)_2CO_3 \rightarrow 2NH_3\uparrow + CO_2\uparrow + H_2O$$

$$NH_3 + H_2O \leftrightarrow NH_4OH \leftrightarrow NH_4^+ + OH^-$$

$$CO_2 + H_2O \leftrightarrow H_2CO_3 \leftrightarrow H^+ + HCO_3^- \leftrightarrow 2H^+ + CO_3^{2-}$$

$$Fe^{3+} + 3OH^- \rightarrow Fe(OH)_3\downarrow \qquad Ni^{2+} + 2HCO_3^- \rightarrow Ni(HCO_3)_2\downarrow$$

$$Fe(OH)_3 + 3Ni(HCO_3)_2 + 6OH^- \rightarrow [Ni_3Fe(OH)_3](CO_3)_3 \cdot 6H_2O + 3CO_3^{2-}.$$

Fig. 3 exhibited the XRD patterns of the products with different hydrothermal treatment times at the ratio of NO_3^-/urea of 3. As being clearly shown in Fig. 3, from 3 h to 48 h, an imperfect structure of NiFe–NO_3-LDH was the unique product and a set of characteristic diffraction peaks appeared at 2θ angles of 9.9°, 19.9° and 34.2°. Here, the absence of other relevant diffraction peaks implies the existence of crystal defect. Nevertheless, these defects of NiFe–NO_3-LDH may be beneficial to its catalytic performance.

3.2. Catalytic behaviors

3.2.1. Catalytic results

Based on the above method, NiFe–NO_3-LDH and NiFe–CO_3-LDH were obtained under the most optimal preparation conditions and used in the synthesis of benzoin ethyl ether via benzaldehyde and ethanol to evaluate their catalytic performance. The conditions of the reaction were as follows: the dosage of NiFe-LDH catalyst being (after pretreatment with N_2 blowing for 2 h) 0.1 g, 3 mL benzaldehyde and 30 mL ethanol; reaction temperature 60 °C and reaction time 60 min. Fig. 4 exhibited the chromatogram analysis of the reaction mixture when the reaction performed for 45 min with NiFe–NO_3-LDH as the catalyst. As it can be seen from the chromatogram, the constituent peaks can be respectively ascribed to ethanol, benzaldehyde and benzoin ethyl ether from left to right. It can be easily confirmed that benzoin ethyl ether was synthesized efficiently from benzaldehyde and ethanol. What's more, the NiFe–NO_3-LDH catalyst could be recycled several times and showed stable activity without structural change. However, when with NiFe–CO_3-LDH as catalyst, the peaks of benzoin ethyl ether did not appear, which witnessed the failed synthesis of benzoin ethyl ether. The catalytic behaviors of these two materials were listed in Table 1. The results evidenced that the synthesis conditions of the catalyst had a profound effect on its corresponding performances.

3.2.2. Plausible mechanism

After investigation, it has been shown that synthesis reaction of benzoin ethyl ether belongs to the acid catalyzed reaction. The reason why benzaldehyde and ethanol, catalyzed by NiFe–NO_3-LDH, can generate benzoin ethyl ether may be of appropriate porous structure and L acid sites of the catalyst. N_2 adsorption/desorption test was performed and the results were given in Fig. 5. The specific surface area

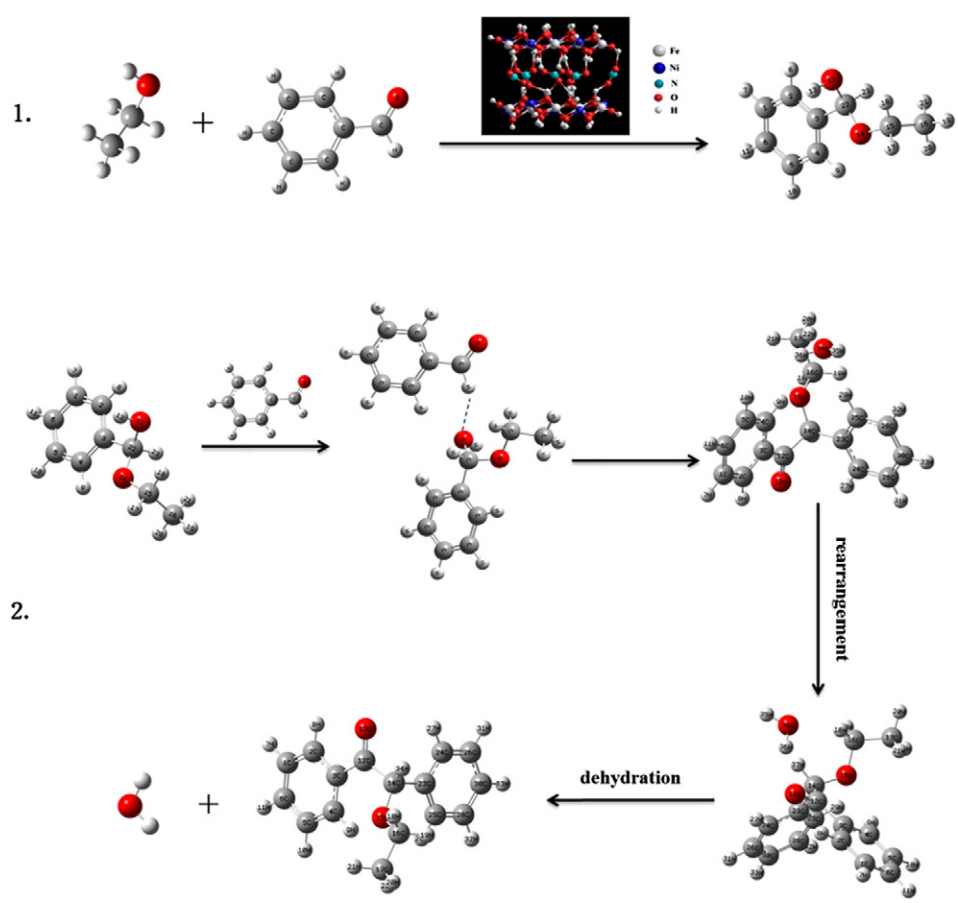

Scheme 2. Plausible mechanism.

of NiFe–NO_3-LDH is 90.56 m^2/g with pore volume of 0.21 cm^3/g. Comparatively, NiFe–CO_3-LDH has relatively smaller surface area (25.01 m^2/g) and pore volume hovering around 0.06 cm^3/g. Generally, larger surface area and pore volume of porous solids in catalytic application are favored to expose the activity as much as possible. Meanwhile, acidic conditions for the synthesis of NiFe–NO_3-LDH will make more unsaturated coordination and crystal defects. Most often, the active sites are located on defect sites associated with low coordination number. In addition, the even wider interlayer space of NiFe–NO_3-LDH endows the reactants with more opportunities to contact with these active sites resulting from the crystal defects. At alkaline synthesis conditions, the hydroxyl ligands will make active site coordination saturation and L acid sites will be masked. Consequently, the ordered array and the resultant high density of basic hydroxyl sites on the basal surfaces made the catalytic activity close to zero [7]. The plausible mechanism is outlined in Scheme 2.

4. Conclusion

In this work, NiFe–NO_3-LDH and NiFe–CO_3-LDH catalysts were prepared at different pH values and aging times, and their catalytic performances were investigated in the one-pot synthesis of benzoin ethyl ether. With NiFe–NO_3-LDH as catalysts, the conversion of benzaldehyde was up to 51.5% and the selectivity of benzoin ethyl ether was nearly 100%. However, the catalytic activity of NiFe–CO_3-LDH was zero.

Acknowledgments

The project was supported by the National Natural Science Foundation of China (50872086), Shanxi Province (2012021006-3), Special/Youth Foundation of Taiyuan University of Technology (2012L022) and Taiyuan Science and Technology (120238).

Appendix A. Supplementary data

Supplementary data to this article can be found online at http://dx.doi.org/10.1016/j.catcom.2014.02.024.

References

[1] F. Bellezza, M. Nocchetti, T. Posati, S. Giovagnoli, A. Cipiciani, J. Colloid Interface Sci. 376 (2012) 20–27.
[2] P. Yang, M. Su, X. Yang, G. Liu, J. Yu, Chin. J. Inorg. Chem. 19 (2003) 485–490.
[3] Z. Xu, J. Zhang, M.O. Adebajo, H. Zhang, C. Zhou, Appl. Clay Sci. 53 (2011) 139–150.
[4] R. Unnikrishnan, S. Narayanan, J. Mol. Catal. A Chem. 144 (1999) 173–179.
[5] J.C.A.A. Roelofs, A.J. van Dillen, K.P. de Jong, Catal. Today 60 (2000) 297–303.
[6] D. Sachdev, M.A. Naik, A. Dubey, B.G. Mishra, Catal. Commun. 11 (2010) 684–688.
[7] X. Lei, F. Zhang, L. Yang, X. Guo, Y. Tian, S. Fu, F. Li, D.G. Evans, X. Duan, AIChE J 53 (2007) 932–940.
[8] R.D. Hetterley, R. Mackey, J.T.A. Jones, Y.Z. Khimyak, A.M. Fogg, I.V. Kozhevnikov, J. Catal. 258 (2008) 250–255.
[9] D. Tichit, M. Naciri Bennani, F. Figueras, R. Tessier, J. Kervennal, Appl. Clay Sci. 13 (1998) 401–415.
[10] D. Tichit, D. Lutic, B. Coq, R. Durand, R. Teissier, J. Catal. 219 (2003) 167–175.
[11] N.T. Thao, H.H. Trung, Catal. Commun. 45 (2014) 153–157.
[12] Y.Z. Chen, C.M. Hwang, C.W. Liaw, Appl. Catal. A Gen. 169 (1998) 207–214.
[13] S. Cadars, G.r. Layrac, C. Gérardin, M.l. Deschamps, J.R. Yates, D. Tichit, D. Massiot, Chem. Mater. 23 (2011) 2821–2831.
[14] Y. Tian, G. Wang, F. Li, D.G. Evans, Mater. Lett. 61 (2007) 1662–1666.
[15] H.S. Shafaat, O. Rudiger, H. Ogata, W. Lubitz, Biochim. Biophys. Acta 1827 (2013) 986–1002.
[16] G. Ovejero, A. Rodriguez, A. Vallet, J. Garcia, Chemosphere 90 (2013) 1379–1386.
[17] S. Leng, X. Wang, X. He, L. Liu, Y.e. Liu, X. Zhong, G. Zhuang, J.-g. Wang, Catal. Commun. 41 (2013) 34–37.
[18] V.R. Choudhary, D.K. Dumbre, Catal. Commun. 12 (2011) 1351–1356.
[19] S. Abelló, E. Bolshak, D. Montané, Appl. Catal. A Gen. 450 (2013) 261–274.
[20] J.M. Thomas, W.J. Thomas, J. Catal. 171 (1997) 349–352.
[21] Y. Li, H. Li, M. Yang, X. He, P. Ni, L. Kang, Z.-H. Liu, Appl. Clay Sci. 52 (2011) 51–55.
[22] H. Li, L. Deng, G. Zhu, L. Kang, Z.-H. Liu, Mater. Sci. Eng. B Solid 177 (2012) 8–13.
[23] F.B. Saiah, B.L. Su, N. Bettahar, J. Hazard. Mater. 165 (2009) 206–217.
[24] X. Lei, L. Yang, F. Zhang, X. Duan, Chem. Eng. Sci. 61 (2006) 2730–2735.
[25] Y. Han, H. Li, X. Ma, Z.-H. Liu, Solid State Sci. 11 (2009) 2149–2155.
[26] S. Vial, V. Prevot, C. Forano, J. Phys. Chem. Solids 67 (2006) 1048–1053.
[27] X. Xie, K. Yan, J. Li, Z. Wang, Catal. Commun. 9 (2008) 1128–1131.
[28] X. Xie, X. An, K. Yan, X. Wu, J. Song, Z. Wang, J. Nat. Gas Chem. 19 (2010) 77–80.
[29] A. Inayat, M. Klumpp, W. Schwieger, Appl. Clay Sci. 51 (2011) 452–459.